A Case of Feline T-cell Lymphoma with Tropism for Striated Muscle and Peripheral Nerve

A feline case of T-cell lymphoma with tropism for the striated muscle and peripheral nerve

M. Mori[*], T. Izawa[*], H. Sasaki[†], J. Sonoyama[†], S. Nishimura[†], S. Shimamura[†], T. Shimada[†], T. Hasegawa[†], M. Kuwamura[*] and J. Yamate[*]

[*] Laboratory of Veterinary Pathology and [†] Veterinary Medical Center, Osaka Prefecture University, 1-58 Rinku Orai Kita, Izumisano, Osaka 598-8531, Japan

Correspondence: T. Izawa

Laboratory of Veterinary Pathology, Osaka Prefecture University, 1-58 Rinku Orai Kita, Izumisano, Osaka 598-8531, Japan

Tel & Fax: +81 72 463 5346

Email: izawa@vet.osakafu-u.ac.jp

Summary

An 11-year-old female American shorthair cat was presented with a 3-month history of ataxia of hind limbs and knuckling of left forelimb. Clinical abnormalities included weight loss, hyperesthesia of the neck and back, cardiac murmur, and systemic muscle atrophy. The cat died 10 days after the initial presentation, and a necropsy was performed. Grossly, extensive pale lesions were seen in the wall of the left ventricle and the septum of the heart. There were no detectable masses in the heart, skeletal muscles and peripheral nerves. Histopathological examination revealed a diffuse, extensive infiltration of atypical lymphoid cells in the heart; the cardiac muscles were severely degenerated, atrophied and replaced by the neoplastic cells. The neoplastic cells with similar morphology were seen in all specimens of the skeletal muscles and peripheral nerves collected at the necropsy. Clonality analysis from the paraffin-embedded heart tissue revealed a monoclonal TCRγ rearrangement. Based on these findings, this case was diagnosed as T-cell lymphoma with tropism for the striated muscle and peripheral nerve.

Keywords: cat; T cell lymphoma; peripheral nerve; striated muscle

Lymphomas are one of the most common malignant neoplasms in cats and commonly affect the gastrointestinal tract, lymph nodes, kidneys and nasal cavity (Valli *et al*., 2016; Taylor *et al*., 2009). Lymphomas rarely infiltrate the peripheral nerve (Mandrioli et al., 2012; Del Grande et al., 2014) or striated muscle (Takeuchi et al., 2010; Jonavicius et al., 2015; Binici et al., 2018), and they can hardly affect both of them in animals and humans. To our knowledge, there is no report of primary skeletal muscle lymphoma in cats. Here we present the first case of feline lymphoma involving the multiple peripheral nerves and multiple striated muscles, including both the skeletal and cardiac muscles.

An 11-year-old female American shorthair cat was presented to Osaka Prefecture University Veterinary Medical Center with a history of ataxia of hind limbs and knuckling of left forelimb that did not respond to steroid therapy for 3 months. The physical examination revealed a weight loss, hyperesthesia of the neck and back, cardiac murmur (Levine 1/6), and systemic muscle atrophy. From the laboratory examination, abnormal findings included leucocytosis (27,600 /μL), anaemia (packed cell volume, 22%; haemoglobin, 7.3 g/dL), and elevated levels of blood urea nitrogen (BUN, 90 mg/dL; normal, 12-41 mg/dL), creatinine (Cre, 2.6 mg/dL; normal, 0.7-2.5 mg/dL), lactate dehydrogenase (264 U/L, normal; <201 U/L). The level of serum creatinine kinase was

51 elevated one day after the initial presentation (>2000 U/L, normal; <469 U/L), and
52 remained higher than normal for four days. Atypical cells were not observed in the
53 peripheral blood. Serological tests for feline leukaemia and feline immunodeficiency
54 viruses were negative. The antibody titre for feline coronavirus was 1,600, suggesting a
55 subclinical infection. A right lateral thoracic radiograph revealed an enlargement of the
56 cardiac silhouette (vertebral heart scale, 9.0; normal,7.5 ± 0.3). B-mode
57 echocardiography showed a moderate hypertrophy in the left ventricular papillary muscle
58 and a left atrium enlargement (LA/AO ratio, 1.61; normal; <1.5). Although the cat
59 received fluid therapy, the general physical condition and increased BUN and Cre were
60 not improved by the therapy. Computed tomography and magnetic resonance imaging
61 could not be performed because of the poor condition. The cat died 10 days after the initial
62 presentation. Necropsy was performed after the carcass was kept frozen for 2 days and
63 then thawed overnight.
64 At necropsy, severe muscle atrophy of the hind limbs was observed. Extensive
65 pale areas were seen in the wall of the left ventricle and the septum of the heart
66 (Supplemental Fig. 1). The right kidney was atrophic, and a dark red nodule of 1 cm in
67 diameter was observed in the adipose tissue around the left kidney. The articular surface
68 of the left humeral head was discoloured (Supplemental Fig. 2). There were no detectable

masses in the heart, skeletal muscles, and peripheral nerves (Supplemental Fig. 3). No macroscopic lesions were detected in the internal organs.

Tissue specimens were collected from the liver, spleen, kidneys, heart, lungs, stomach, small and large intestines, trachea, pancreas, adrenal glands, lymph nodes (mesenteric), bone marrow, eyes, skeletal muscles (femoral, back, lingual, anal sphincter and ocular muscles), humeral head, brain, spinal cords at the levels of L3, L5, C1 and C5, and peripheral nerves (plexus brachialis, sciatic and spinal root nerves). They were fixed in 10% neutral-buffered formalin, routinely processed, embedded in paraffin, cut at 5 μm, and stained with haematoxylin and eosin (HE). Sections were also subjected to immunohistochemistry (IHC) with primary antibodies specific for CD3 and CD20 as listed in Table 1. After dewaxing and pretreatment, tissue sections were immunostained in a Histostainer™ system (Nichirei Biosciences, Tokyo, Japan). Briefly, sections were treated with 5% skimmed milk in phosphate buffered saline (PBS) for 10 min and reacted with each primary antibody for 1 h. After incubation in 3% H_2O_2 for 15 min, application of horseradish peroxidase-conjugated secondary antibody (Histofine Simple Stain MAX PO®; Nichirei Biosciences) for 30 min was performed. Positive reactions were visualized with 3,3'-diaminobenzidine (DAB substrate kit; Nichirei Biosciences). Sections were counterstained lightly with haematoxylin. Non-immunized mouse or rabbit IgG was

87 substituted for primary antibody as a negative control. Infiltrating lymphocytes in the
88 same section served as an internal positive control.

89 Histopathological examination revealed a diffuse, extensive infiltration of round
90 neoplastic cells with round to ovoid nuclei and scant eosinophilic cytoplasm in the heart
91 (Figs. 1 and 2). The cardiac muscles were severely fragmented, atrophied and replaced
92 by the neoplastic cells. Cellular and nuclear atypia were moderate (Supplemental Fig. 4).
93 Mitotic figures were often seen (31 per 10 high-power fields). Some neoplastic cells were
94 positive for CD3 (Supplemental Fig. 5), whereas they were negative for CD20
95 (Supplemental Fig. 6). Clonality analysis was performed from the paraffin-embedded
96 tissue of the heart in which the neoplastic involvement was most extensive. The result
97 showed a monoclonal TCRγ rearrangement (Supplemental Fig. 7). Therefore, the cardiac
98 lesion was diagnosed as T-cell lymphoma.

99 The neoplastic cells with similar morphology were seen in all specimens of the
100 skeletal muscles (Fig. 3 and Supplemental Fig. 8) and peripheral nerves (Fig. 4 and
101 Supplemental Fig. 9) collected at the necropsy. The neoplastic cells were also seen in the
102 dark red nodule in the adipose tissue around the left kidney and the gastric mucosa.
103 However, neoplastic cells were not observed in the central nervous system, kidneys,
104 intestines or lymph nodes. Histopathological findings in other organs included bile duct

105 cystadenoma in the liver and chronic nephropathy. There were extensive loss and
106 degeneration of articular cartilage, decrease in bone marrow cells and mild fibrosis in the
107 medullary cavity in the left humeral head, while the right humeral head was intact.

108 Based on these findings, this case was diagnosed as T-cell lymphoma with
109 tropism for the striated muscle and peripheral nerve. Lymphomas primarily involving the
110 striated muscle or peripheral nerve are rare, but are reported in humans, dogs and cats.
111 Human lymphomas very rarely involve both the peripheral nerve and skeletal muscle
112 (Advani *et al*., 2015). In humans, peripheral nerve or skeletal muscle lymphomas tend to
113 infiltrate along the anatomic structure, and peripheral nerve lymphomas typically do not
114 invade the central nervous system from the cranial or peripheral nerve roots (Oya, 2014).
115 Some types of lymphomas are expected to have affinity for the peripheral nerves or
116 skeletal muscles. In humans, primary peripheral nerve lymphomas are mostly diffuse
117 large B-cell lymphoma (Misdraji *et al*., 2000). The patients have ataxia, hyperesthesia,
118 pain and muscle atrophy caused by the infiltration of lymphoma into the peripheral nerves.
119 Skeletal muscle lymphomas are rarer than peripheral nerve lymphomas. In human skeletal
120 muscle lymphomas, B-cell lymphomas are the most common, although natural killer
121 lymphoma, T cell lymphoma, and Hodgkin’s disease have been also described to involve
122 the muscle (Surov, 2014). Clinical symptoms of the skeletal muscle lymphomas include

123 pain, muscle atrophy, paraesthesia and ataxia. In the present case, the clinical symptoms
124 such as ataxia of hind limbs, knuckling of left forelimb, hyperesthesia of the neck and
125 back, and muscle atrophy was thought to be caused by the involvement of the lymphoma
126 to the peripheral nerves and skeletal muscles.

127 Since the present lymphoma did not form mass in any organ, it was difficult to
128 diagnose this case as lymphoma before necropsy. Some human cases have masses or
129 swelling of peripheral nerves (Agrawal *et al*., 2013) and skeletal muscles (Matikas *et al*.,
130 2013), while others have no apparent masses and are detectable only after biopsy or
131 necropsy (Asanome *et al*., 2018). In cats, B-cell lymphoma in the multiple peripheral
132 nerves (e.g. sciatic nerve, multiple brachial plexus) without mass formation was reported
133 (Higgins *et al*., 2008). Thus neurotropic lymphoma should be considered in the
134 differential diagnosis when an animal presents neurological symptoms such as ataxia and
135 hyperesthesia.

136 In this case, myocardial injury by the lymphoma was severe and extensive, and
137 thus was considered to be the major cause of death. Primary cardiac tumours are
138 uncommon in the dogs and cats and lymphomas infrequently involve the heart (Treggiari
139 *et al*,. 2017). Cardiac neoplasms can cause severe, life-threatening clinical signs with
140 short median survival times. Canine T-cell lymphoma with prominent cardiac and

peripheral nerve involvement (Nakagun *et al*., 2018) and feline primary cardiac lymphoma (Shinohara *et al*., 2005) were reported in the veterinary literature. The canine case had an enlargement of the cardiac silhouette and shares many similarities with this case, including the involvement of the heart and multiple peripheral nerves, clinical signs (e.g. hindlimb ataxia), and T-cell monoclonality; however, skeletal muscle involvement was not detected in the canine case.

The carcass was kept frozen for 2 days and then thawed overnight before the necropsy in this case. Immunoreactivity can be weakened in the previously frozen tissue for certain antibodies (Edgerton *et al*., 2000). The smaller portion of CD3-positive neoplastic cells in this case than routine necropsy samples could be the result of the freezing and thawing. Given the result of the clonality analysis from the same paraffin-embedded heart tissue, genomes are considered to be more tolerant to freezing and thawing than antigens.

In summary, to the best of our knowledge, this is the first report of feline lymphoma involving both the striated muscle and peripheral nerve. The present case would contribute to further understanding of the biological and pathological features of lymphomas in animals.

Conflict of interest statement

The authors declare no conflicts of interest with respect to the publication of this manuscript.

References

Advani P, Jiang L, Srinivasan S, Foran J. (2015) Disseminated extranodal marginal zone lymphoma involving the gastrocnemius muscle with sural neurolymphomatosis. *Annals of Hematology*, **94**, 1939-1940.

Agrawal S, Gi MT, Ng SB, Puhaindran ME, Singhania P. (2013) MRI and PET-CT in the diagnosis and follow-up of a lymphoma case with multifocal peripheral nerve involvement. *Diagnostic and Interventional Radiology*, **19**, 25-28.

Asanome A, Kano K, Takahashi K, Saito T, Sawada J et al. (2018) A case of neurolymphomatosis that was diagnosed by acoustic nerve biopsy. *Clinical Neurology*, **58**, 93-99.

Binici DNR, Karaman A, Timur O, Tasar PNT, Sanibas AV. (2018) Primary skeletal muscle lymphoma: A case report. *Molecular and Clinical Oncology*, **8**, 80-82.

Del Grande A, Sabatelli M, Luigetti M, Conte A, Granata G et al. (2014) Primary multifocal lymphoma of peripheral nervous system: case report and review of the

177 literature. *Muscle & Nerve*, **50**, 1016-1022.

178 Edgerton ME, Roberts SA, Montone KT. (2000) Immunohistochemical performance of
179 antibodies on previously frozen tissue. *Applied Immunohistochemistry & Molecular*
180 *Morphology*, **8**, 244-248.

181 Higgins MA, Rossmeisl JH Jr, Saunders GK, Hayes S, Kiupel M. (2008) B-cell
182 lymphoma in the peripheral nerves of a cat. *Veterinary Pathology*, **45**, 54-57.

183 Jonavicius K, Salcius K, Meskauskas R, Valeviciene N, Tarutis V et al. (2015) Primary
184 cardiac lymphoma: two cases and a review of literature. *Journal of Cardiothoracic*
185 *Surgery*, **10**, 138.

186 Mandrioli L, Morini M, Biserni R, Gentilini F, Turba ME. (2012) A case of feline
187 neurolymphomatosis: pathological and molecular investigations. *Journal of Veterinary*
188 *Diagnostic Investigation*, **24**, 1083-1086.

189 Matikas A, Oikonomopoulou D, Tzannou I, Bakiri M. (2013) Primary abdominal muscle
190 lymphoma. *BMJ Case Reports*, doi: 10.1136/bcr-2012-008311.

191 Misdraji J, Ino Y, Louis DN, Rosenberg AE, Chiocca EA et al. (2000) Primary lymphoma
192 of peripheral nerve: report of four cases. *The American Journal of Surgical Pathology*,
193 **24**, 1257-1265.

194 Nakagun S, Horiuchi N, Watanabe K, Matsumoto K, Tagawa M et al. (2018) CD3 and

195 CD20 co-expression in a case of canine peripheral T-cell lymphoma with prominent
196 cardiac and peripheral nerve involvement. *Journal of Veterinary Diagnostic Investigation*,
197 **30**, 779-783.
198 Oya Y. (2014) Lymphoma in the peripheral nerves and muscles. *Brain and Nerve*, **66**,
199 955-967.
200 Shinohara N, Macgregor JM, Calo A, Rush JE, Penninck DG et al. (2005) Presumptive
201 primary cardiac lymphoma in a cat causing pericardial effusion. *Journal of Veterinary*
202 *Cardiology*, **7**, 65-69.
203 Surov A. (2014) Imaging findings of skeletal muscle lymphoma. *Clinical Imaging*, **38**,
204 594-598.
205 Takeuchi Y, Fujino Y, Goto-Koshino Y, Ohno K, Uchida K et al. (2010) Long term
206 survival of primary skeletal muscle lymphoma in a miniature dachshund. *Journal of*
207 *Veterinary Medical Science*, **72**, 673-677.
208 Taylor SS, Goodfellow MR, Browne WJ, Walding B, Murphy S et al. (2009) Feline
209 extranodal lymphoma: response to chemotherapy and survival in 110 cats. *Journal of*
210 *Small Animal Practice*, **50**, 584-592.
211 Treggiari E, Pedro B, Dukes-McEwan J, Gelzer AR, Blackwood L. (2017) A descriptive
212 review of cardiac tumours in dogs and cats. *Veterinary and Comparative Oncology*, **15**,

273-288.

Valli VEO, Kiupel M, Bienzle D. (2016) Hematopoietic system. In: *Jubb, Kennedy, and Palmer`s Pathology of Domestic Animals*, 6th Edit., MG Maxie, Ed., Elsevier Saunders, Philadelphia, pp. 239-241.

Figure legends

Fig. 1

There is a diffuse, extensive infiltration of basophilic neoplastic lymphoid cells in the heart. L; wall of the left ventricle, R; wall of the right ventricle, S; ventricular septum. HE. Bar, 5 mm

Fig. 2

The cardiac muscles are severely degenerated, atrophied and replaced by the neoplastic lymphoid cells. HE. Bar, 50 μm

Fig. 3

There is focal, dense infiltration of the neoplastic lymphoid cells in the femoral muscle with a marked muscle atrophy. HE. Bar, 100 μm

231

232 Fig. 4

233 There is focal, dense infiltration of the neoplastic lymphoid cells in the plexus brachialis.

234 Nerve fibres are fragmented and replaced by the neoplastic cells. Note the presence of

235 less affected nerve bundles (at the right top). HE. Bar, 100 μm

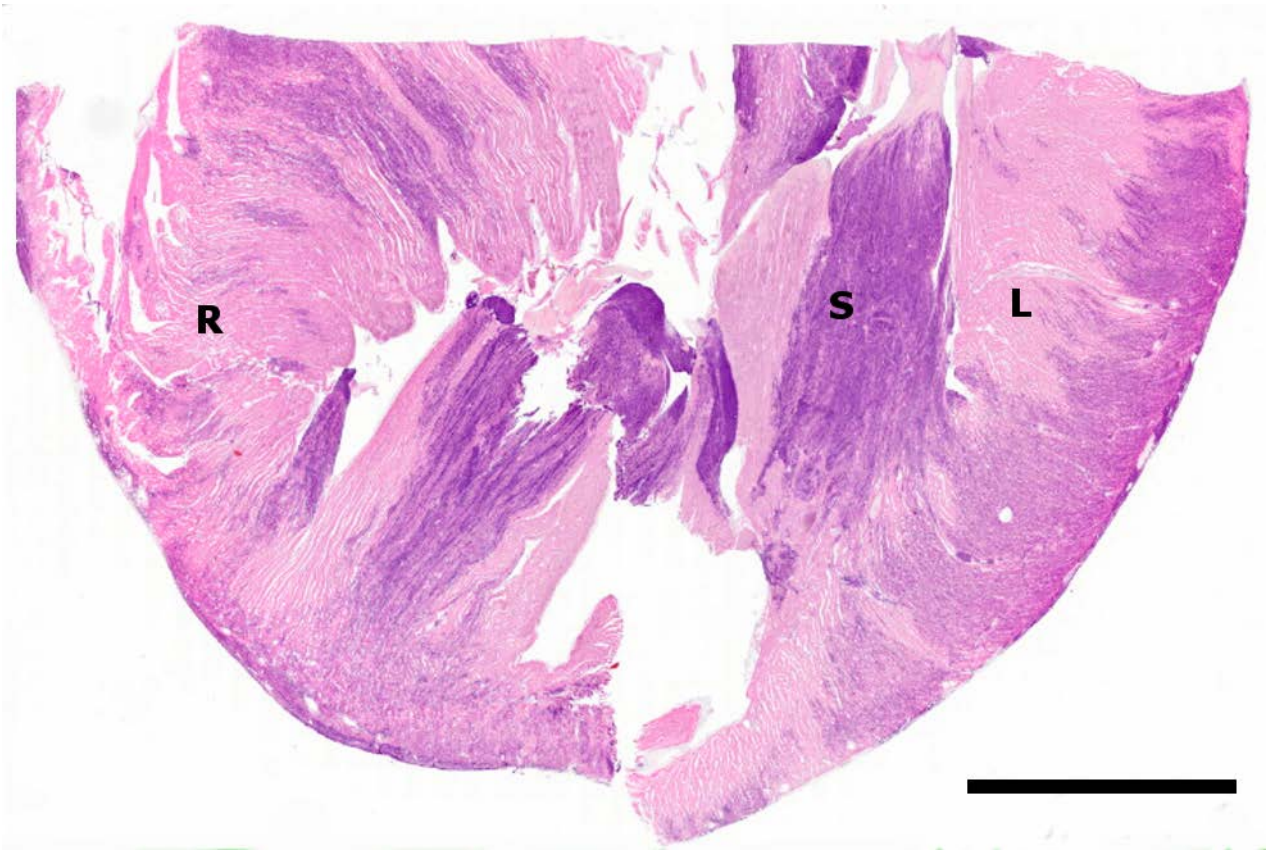

Fig. 1

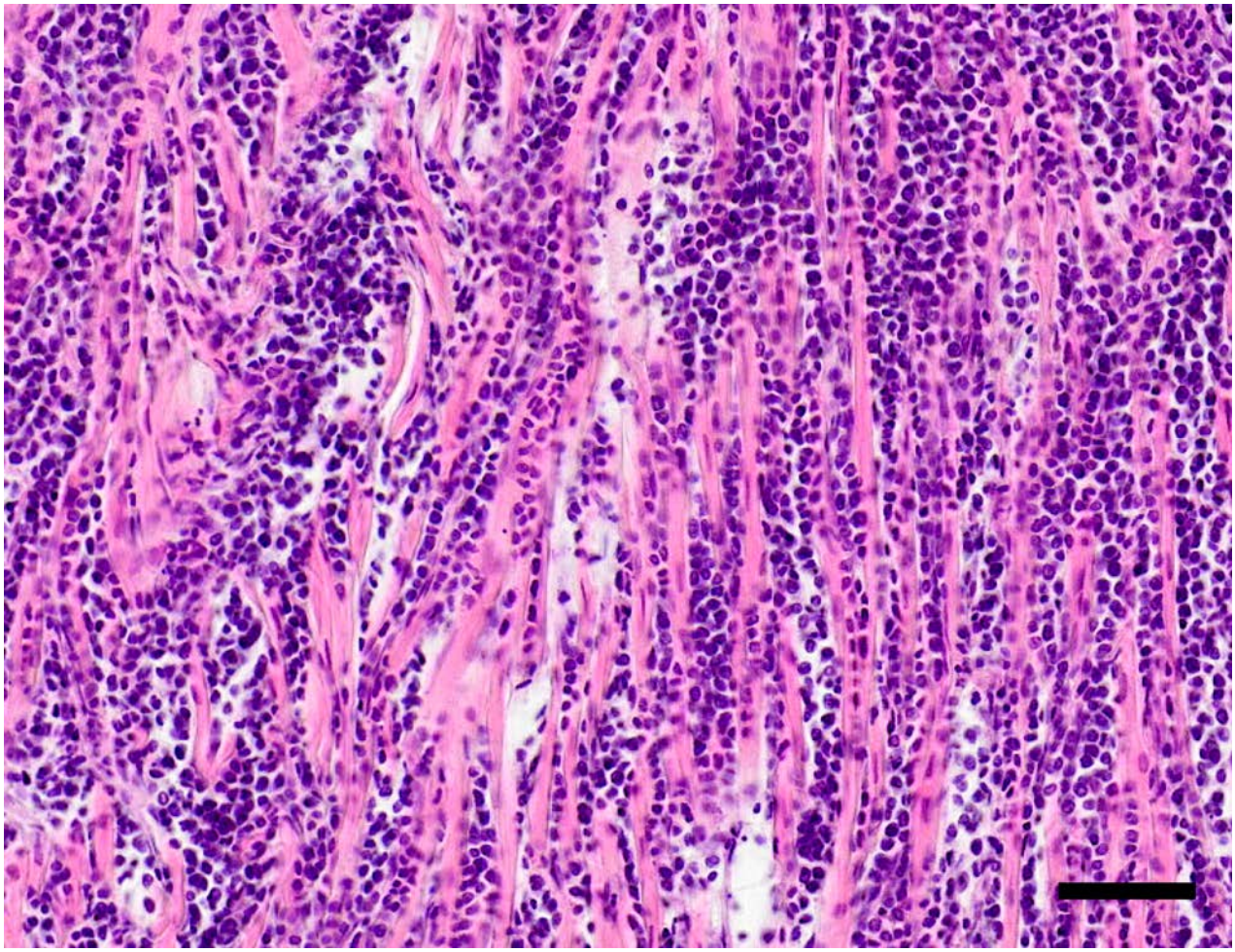

Fig. 2

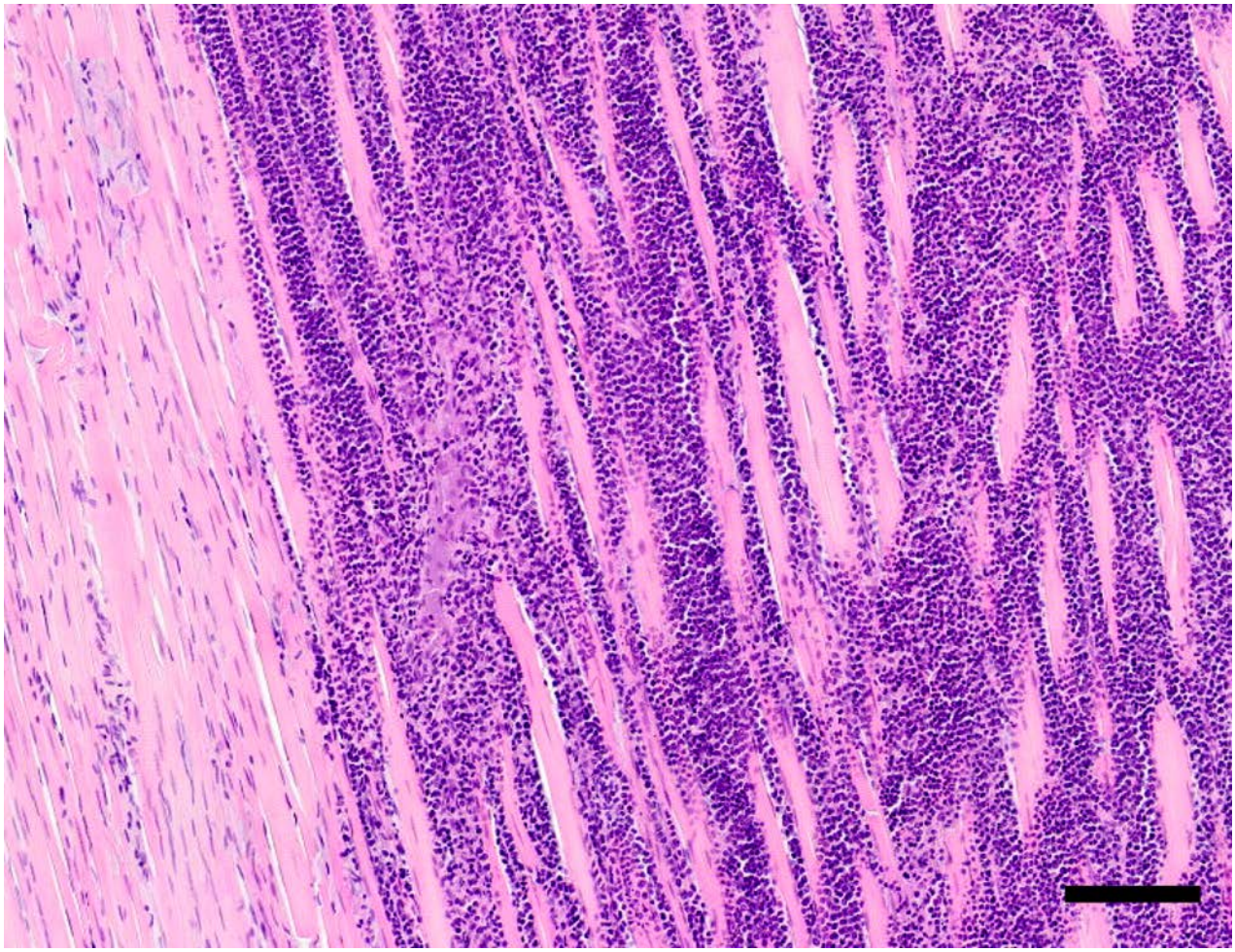

Fig. 3

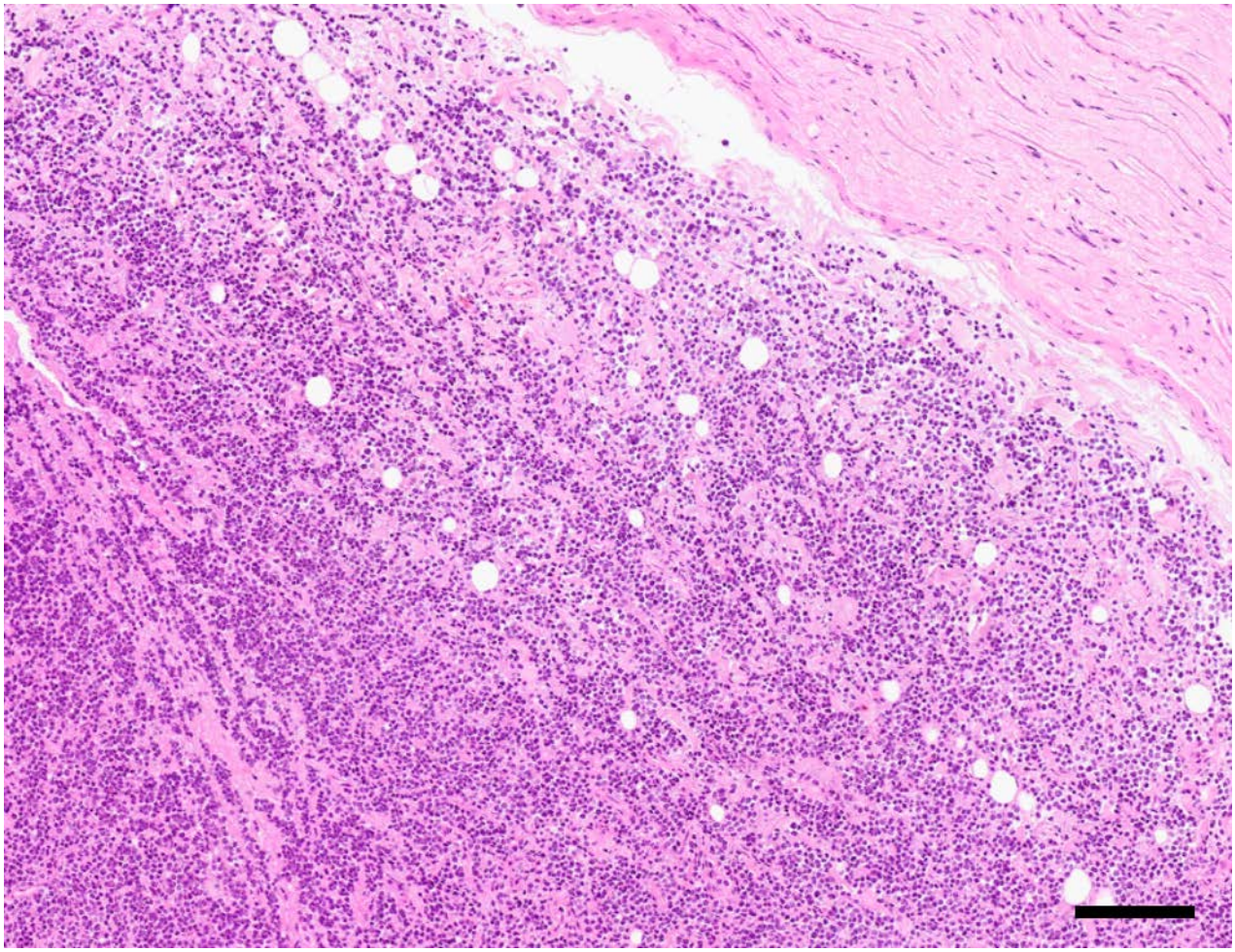

Fig. 4

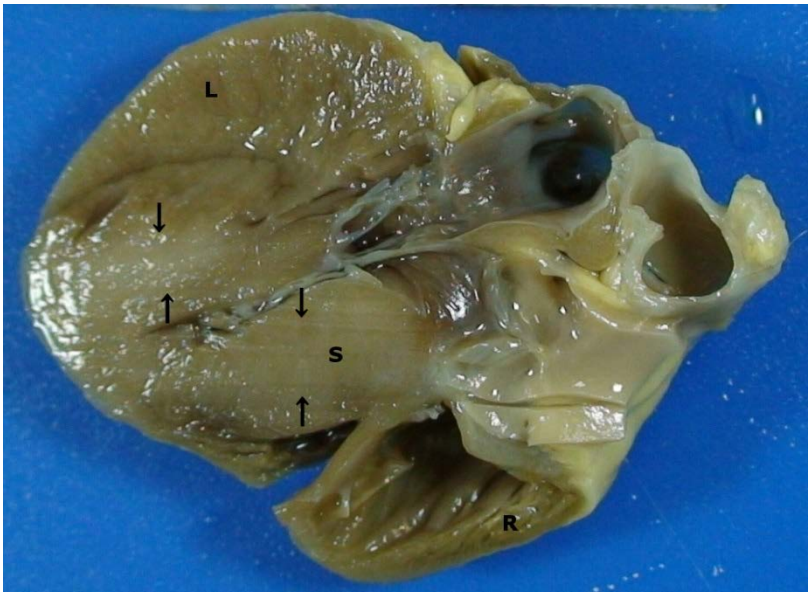

Supplemental Fig. 1. Extensive pale areas are seen in the wall of the left ventricle and the septum of the heart (arrows). L; left ventricle wall, R; right ventricle wall, S; ventricular septum.

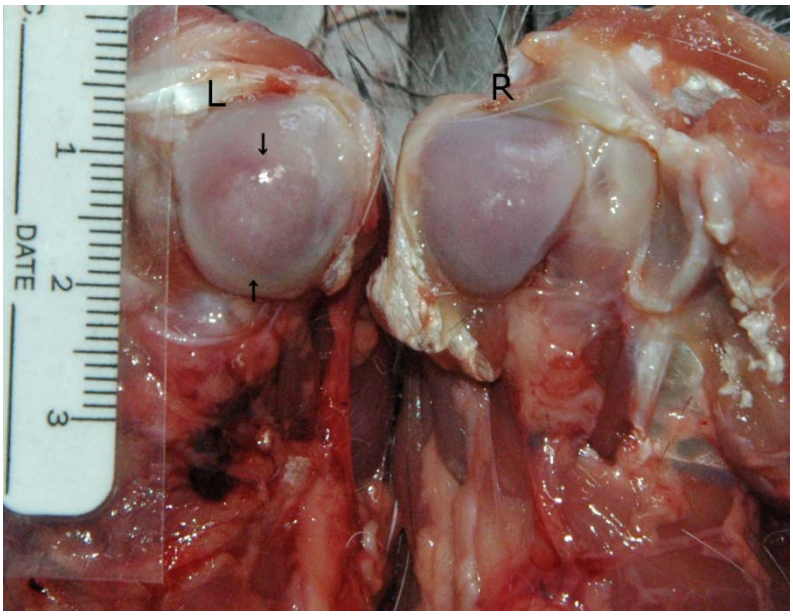

Supplemental Fig. 2. The articular surface of the left humeral head was discoloured (arrows) compared with the contralateral surface. L; left, R; right.

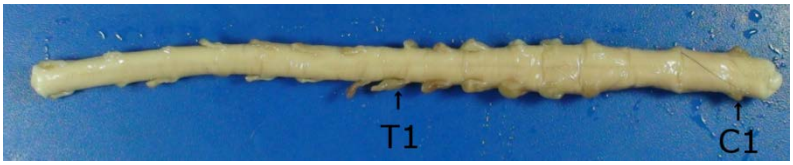

Supplemental Fig. 3. There were no detectable masses in the spinal root nerves. C1; cervical nerve 1, T1; thoracic nerve 1.

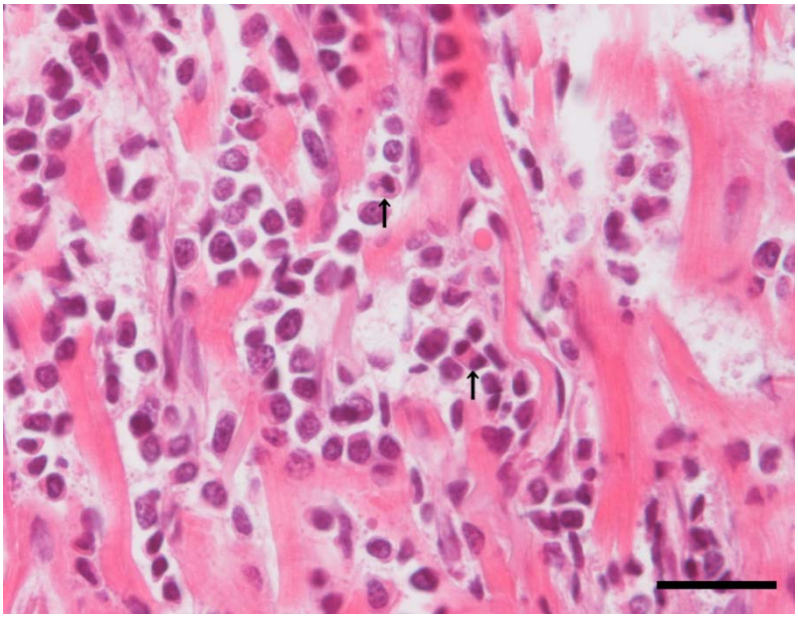

Supplemental Fig. 4. Moderate cellular and nuclear atypia of the lymphoid neoplastic cells in the heart. Arrows indicate mitotic figures. Note the presence of degenerated and atrophied cardiac muscles. HE. Bar, 500 μm

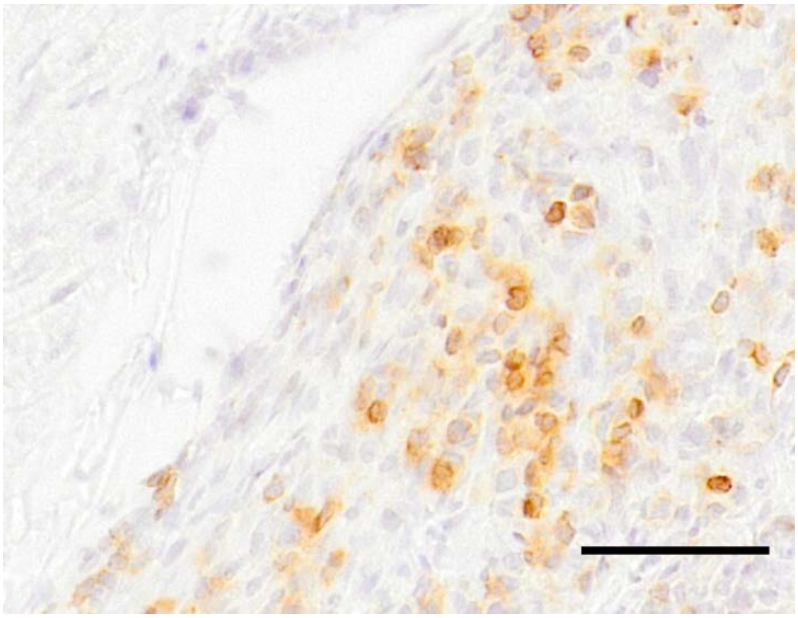

Supplemental Fig. 5. Some neoplastic cells are positive for CD3. Heart. IHC counterstained with hematoxylin. Bar, 50 μm

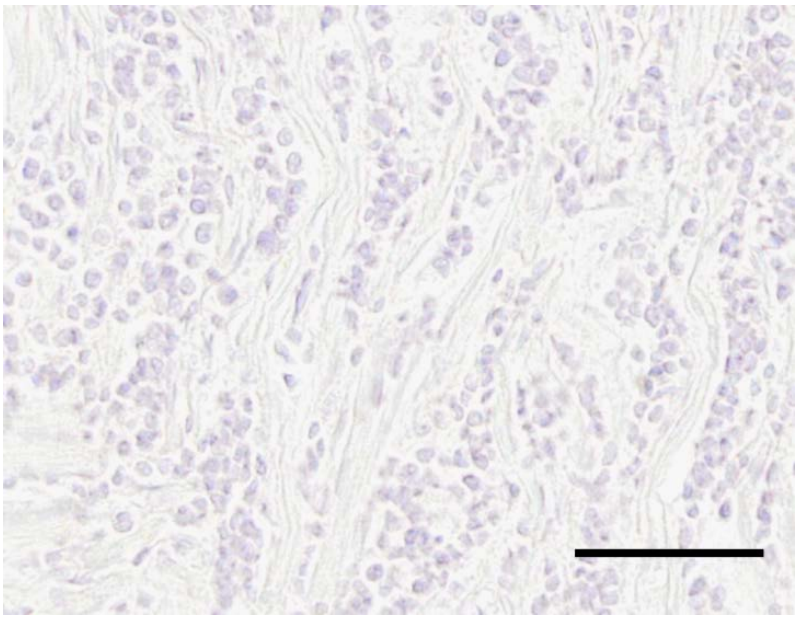

Supplemental Fig. 6. Neoplastic cells are negative for CD20. Heart IHC counterstained with hematoxylin. Bar, 50 μm

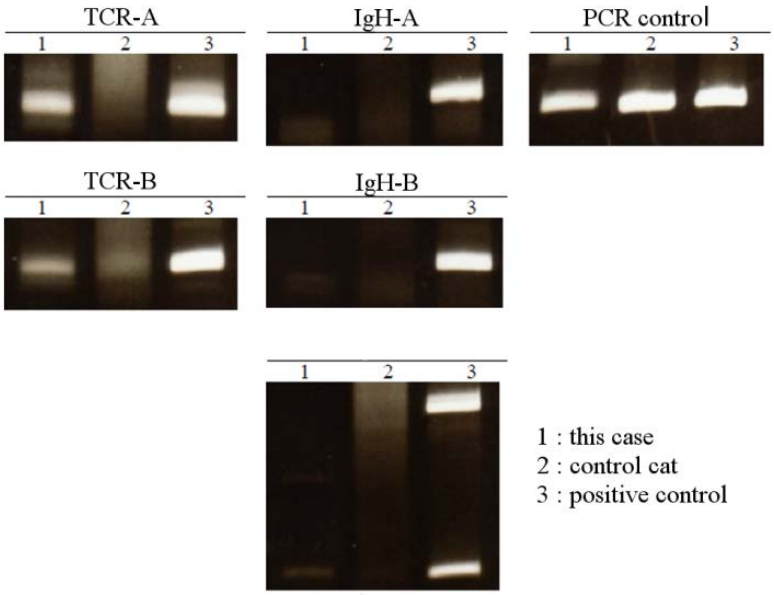

Supplemental Fig. 7. Clonality analysis from the paraffin-embedded heart sample indicates a monoclonal TCRγ rearrangement.

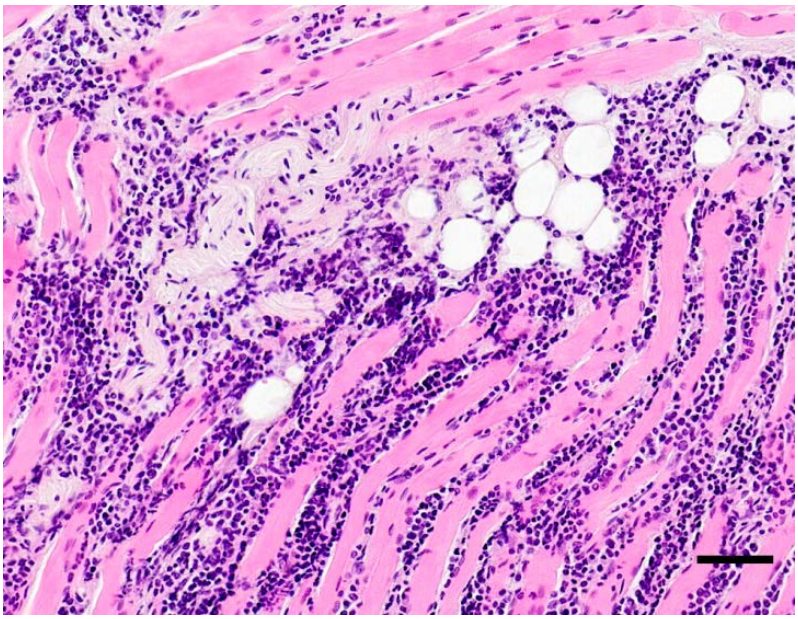

Supplemental Fig. 8. The atypical lymphoid cells are seen in the lingual muscle. HE. Bar, 50 μm

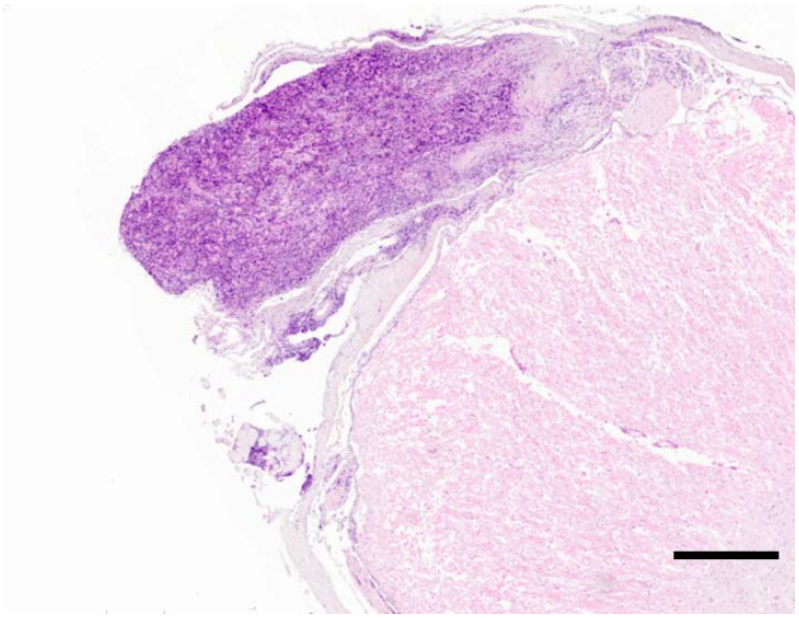

Supplemental Fig. 9. The atypical lymphoid cells are seen in the spinal root nerves. Transvers section of the spinal cord at C1 level. HE. Bar, 500 μm